Effect of Topography on Glossiness and Surface Color for a 5052 Aluminum Alloy[*1]

Makiko Yonehara[1,*2], Koichiro Kihara[2], Yoshihito Kagawa[2],
Hiroaki Isono[3] and Toshio Sugibayashi[2]

[1]*Graduate School of Engineering, Takushoku University, Hachioji 193-0985, Japan*
[2]*Department of Mechanical System Engineering, Faculty of Engineering, Takushoku University, Hachioji 193-0985, Japan*
[3]*Department of Precision Mechanical System Engineering, Polytechnic University, Sagamihara 229-1196, Japan*

The effect of topography on the glossiness and surface color of aluminum alloy A5052 specimens was experimentally investigated. The surfaces of the specimens were machined using either a vertical milling machine, a horizontal milling machine or a shaping machine. Four specimens were produced by each machine so that the arithmetical mean roughness value, *Ra*, was less than 1 μm under four different cutting conditions. The experimental results revealed that the vertical and horizontal milling glossiness values were nearly the same, while the glossiness values of the shaped surface was less than half of this value. The surface color of all of the specimens was gray, although the lightness value of the surface color, L^*, for the horizontal milling surface had the highest value. Based on the experimental results, it was determined that the surface texture of specimens produced by these machines could be characterized by their glossiness and surface color. These results could prove an effective indicator for choosing the most appropriate machining method by providing surface texture values.

1. Introduction

In recent years, diversification and functional enhancements to industrial products has led companies to improve the competitiveness of a product by upgrading its physical appearance.[1] An industrial product's appearance is strongly dependent upon the textures of its constituent materials. The texture of a material is primarily determined by the mechanical processing that the material experiences during the manufacturing of the product.[2] Surface texture is determined by several factors in surface formation, but the final evaluation performed by a customer's vision. In fact, a standard sample is used to evaluate surface texture during the manufacturing process, and this evaluation is frequently determined by a test based on the human eye.[3,4]

In the current design of industrial products, the texture of a surface is called the "surface texture." The method for designing a surface texture is standardized by JIS B 0031:2003. The standardized method is solely concerned with the surface roughness resulting from the processing applied to the surface, and is defined by the surface roughness in terms of the arithmetical mean roughness, *Ra*. However, even if two surfaces have practically the same roughness in terms of *Ra*, the surfaces themselves may differ considerably depending on the processing methods, processing conditions and processing tools applied to the surfaces.[5,6] To evaluate the surface texture more accurately, it is necessary to also account for relevant factors in addition to the arithmetical mean roughness, *Ra*.

A number of previous studies dealing with the proper evaluation of surface texture have explained the relationship between surface roughness and the specular reflected light[7] or the relationship between surface roughness and the intensity of scattered light.[8,9] These studies measured the intensity of the reflected light, but rarely paid any attention to the wavelength of the reflected light, that is, the surface color, and its relationship with surface roughness. In previous experimental studies, the authors explored how to evaluate surface texture properly, paying attention to how the roughness, glossiness, and color are interrelated in the determination of surface texture for a polished surface. These studies revealed that it is possible to evaluate surface texture accurately by utilizing these three factors.[10]

In some of the studies that evaluated the surface texture of an aluminum alloy, the surface of the aluminum alloy specimen was prepared by extrusion molding or die-casting die surface.[11,12] On the other hand, other studies, including studies conducted by the authors, investigated the surfaces of aluminum alloy specimens processed by a milling machine or by blast processing.[13] However, there have been only a few studies that have explored aluminum alloy surfaces that have mechanically processed with different methods, and, thus, have different surface roughness characteristics from the viewpoint of elucidating the relative involvement of the three factors, *i.e.*, surface roughness, glossiness and color, in the determination of surface textures.[14]

In this study, the surfaces of specimens made from an aluminum alloy were processed with a vertical milling machine (hereafter "vertical milling"), a horizontal milling machine (hereafter "horizontal milling") and a shaper. The effects of surface topography on glossiness and surface color were experimentally investigated using these specimens to evaluate the surface textures of different surface topographies.

2. Experimental Method

2.1 Surface processing and roughness

The specimens used in this experiment were made from aluminum alloy A5052 whose chemical composition is

---

Table 1　Chemical compositions.

Alloy no.	Si	Fe	Cu	Mn	Mg	Cr	Zn	Ti	Others		Al
									Each	Total	(%)
A5052	0.09	0.27	0.02	0.02	2.45	0.20	0.00	0.01	0.05 max.	0.15 max.	Residual

shown in Table 1.[15] Tensile tests were performed on test pieces taken in both parallel and the orthogonal directions for the rolling direction at JIS13B, in order to investigate the mechanical properties of the specimens. Tensile strength in the direction parallel to the rolling direction was found to be about 250 MPa, the proof stress is about 189 MPa, and the Young's modulus is about 69 GPa. In the tensile direction, the parallel (length) direction is set to x, the direction of a right angle (width) is y and the thickness direction of the test piece is set to z. Poisson's ratio is almost equal to $|\varepsilon_y/\varepsilon_x| = 0.36$ and $|\varepsilon_z/\varepsilon_x| = 0.35$. On the other hand, tensile strength for direction orthogonal to the rolling direction was found to be about 242 MPa, the proof stress is about 186 MPa, and the Young's modulus is about 71 GPa. In this orientation, Poisson's ratio is almost equal to $|\varepsilon_y/\varepsilon_x| = 0.35$ and $|\varepsilon_z/\varepsilon_x| = 0.33$. Furthermore, the hardness of the upper surface of a specimen, the undersurface, and the four sides were measured with a Vickers hardness testing machine. The results coincided with those in 77-82HV0.3/15. The specimens used in this experiment can be regarded as isotropic.

Each specimen was a rectangular piece having a surface area of 70×70 mm and a thickness of 5 mm. A vertical mill, a horizontal mill, and a shaper were used to change the topography of the specimens. Both vertical and horizontal milling systems have a knee that moves up and down along a column. The table rides through a saddle on the knee and uses the milling machine structure to move right and left. Vertical milling has the principal axis of the milling machine perpendicular to the specimen, and horizontal milling has the principal axis parallel to the specimen. A shaping machine intermittently moves the table in a right-angled direction to the ram. Furthermore, the byte attached to the ram reciprocates and the planning and slotting of the work are performed.[16]

The cutting conditions are shown in Table 2. The processing of each surface was adjusted to provide three different surfaces with roughness $Ra \leq 1.0$ μm, but different from each other. Specimen No. 1 had the surface with the smallest Ra, and Specimen No. 3 had the highest. Vertical processing was achieved by a milling machine equipped with a 120 mm diameter face cutter with an attached carbide tip. Horizontal processing was achieved by a milling machine equipped with a 60 mm diameter plane cutter containing 14 high speed steel blades. The shaper's cutter was made of high speed steel. Specimens No. 1 and No. 2 were processed with a spring-necked turning tool and specimens No. 3 and No. 4 were processed with a goose-necked turning tool.

The roughness of each specimen was determined with a stylus profilometer SV-624 (Mitutoyo Corp). For each measurement, the cut-off value was set at 0.8 mm and the measurement length was 4 mm. The surfaces processed

Table 2　Cutting conditions.

Specimen No.		1	2	3	4
Vertical milling	Revolution (rpm)	610	610	610	610
	Cutting speed (m/min)	300	300	300	300
	Feed speed (mm/min)	30	100	300	500
	Feed (mm/teeth)	0.05	0.16	0.49	0.82
Horizontal milling	Revolution (rpm)	620	225	225	225
	Cutting speed (m/min)	117	42	42	42
	Feed speed (mm/min)	15	50	100	150
	Feed (mm/teeth)	0.0017	0.016	0.032	0.048
Shaping	Cutting speed (m/min)	4.8	4.8	4.8	4.8
	Feed (mm/teeth)	0.31	0.91	0.15	0.31

by vertical milling and the shaper were measured in a direction perpendicular to the cutting direction. The surfaces processed by horizontal milling were measured in a direction parallel to the cutting direction. Measurements were performed along three parallel lines with a 5 mm interval between adjacent lines on a central portion of the surface. The roughness of a surface was calculated as the average of the three measurements.

2.2　Measurement of surface glossiness and color

The surface glossiness measurements were conducted with a gloss meter (mirror-TRI-gloss, BYK-Gardner). The incident angle from the light source, a white light having spectral characteristic of a CIE standard illuminant C, was set at $60°$. A photo-receptor was set so that its aperture was 4.4 ± 0.1 degrees in a plane parallel to the incident light plane and 11.7 ± 0.2 degrees in a plane normal to the incident light plane. The glossiness measurements were taken in a manner similar to the surface roughness measurements: three parallel lines along the central portion of the specimen surface.

The surface color measurements were carried out with a spectral colorimeter (CM-2600d, Minolta). The light source was set to irradiate white light with the same spectral characteristics as the one used in the glossiness measurement.

A 3 mm diameter circular light spot was applied to five different sites on the specimen surface: one site at the center, two sites arranged along a line passing through center with the center positioned 5 mm away from the sites, and two sites similarly arranged along a line normal to the former line. The measurements from the five sites were averaged for each specimen, and the average was assumed to represent the color of the surface according to CIELAB color space (JIS Z 8729:2004). It should be noted that all specimens were washed with acetone before the test to remove grease and dust.

3. Results and Observations

3.1 Relationship between surface roughness and glossiness

The representative appearances and roughness profiles of surfaces processed by vertical milling, horizontal milling and the shaper are shown in Figs. 1(a) through (d). An illustration of the processing method is displayed in Fig. 1. The solid line arrow in each figure represents the cutting direction and the dashed line arrow depicts the coarseness curve measurement direction. Figure 1(c) shows the roughness profile for the
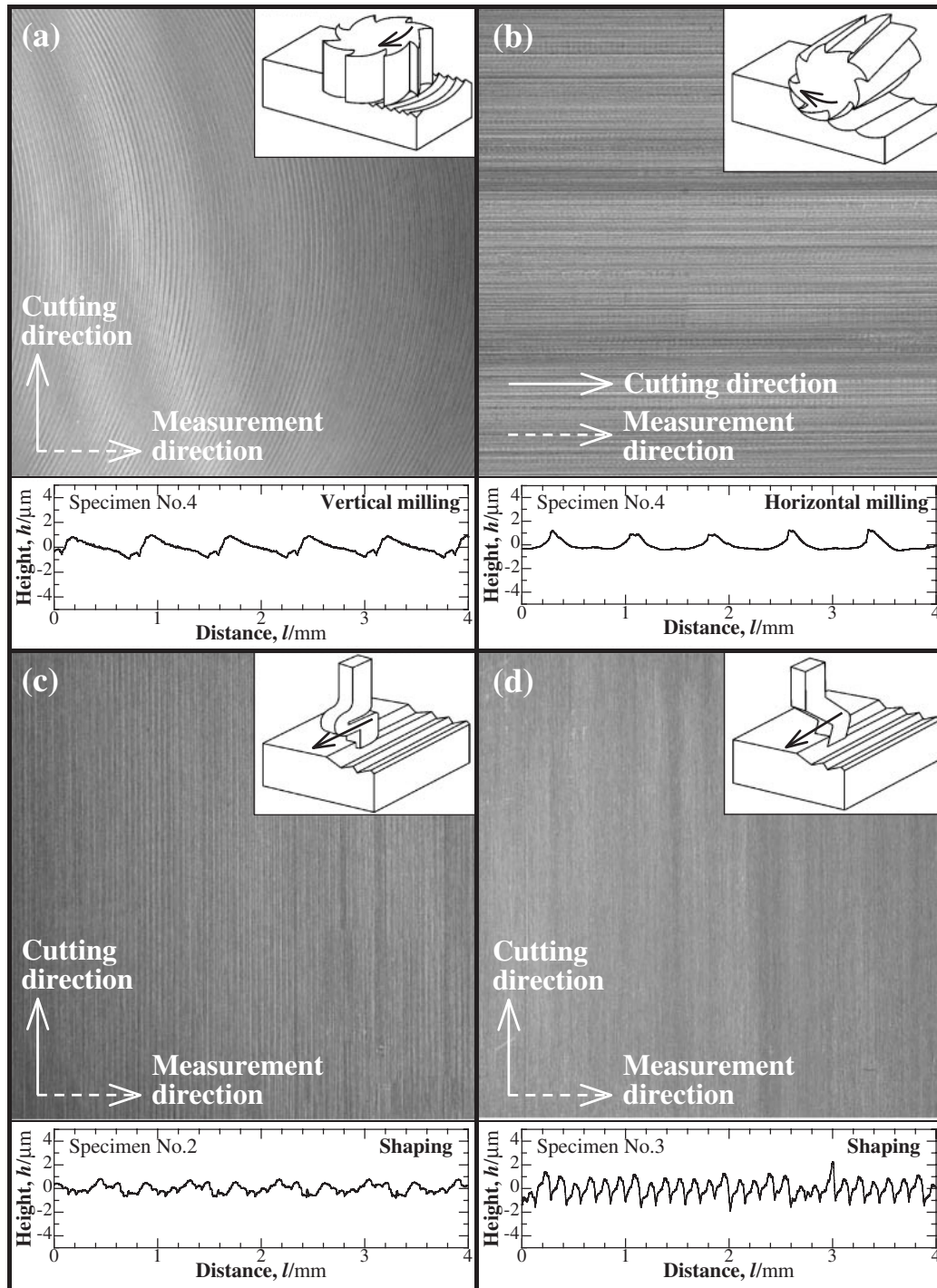

Fig. 1 Photographs and roughness profiles: (a) Vertical milling, (b) Horizontal milling, (c) Shaping (spring-necked turning tool) and (d) Shaping (goose-necked turning tool).
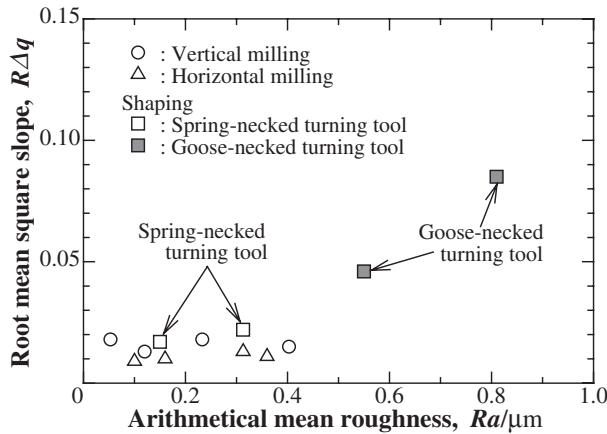
Fig. 2 Relationship between arithmetical mean roughness Ra and root mean square slope $R\Delta q$.

Fig. 3 Relationship between arithmetical mean roughness Ra and glossiness $Gs(60°)$.

surface processed by the shaper with the spring-necked turning tool, while Fig. 1(d) shows the corresponding profile when the shaper was equipped with the goose-necked turning tool. The surface profiles reflect the characteristics of their respective processing methods. The profile of the surface processed by the vertical milling is shown in Fig. 1(a). The surface has a saw-tooth like profile. The profile of the surface processed by the horizontal milling is shown in Fig. 1(b). This surface has a concave-indentation profile. Finally, the profiles of the surfaces processed by the shaper equipped with the spring-necked turning tool and the goose-necked turning tool are shown in Figs. 1(c) and (d). These surfaces exhibit a wavy profile with a comparatively short cycle length and a trapezoidal convex elemental profile.

For each specimen surface, the relationship between Ra and $R\Delta q$, or the root mean square of slopes that represents the average slope of indentations of the surface, is shown in Fig. 2. When the arithmetical mean roughness, Ra, was about $Ra \leq 0.4\,\mu m$, the $R\Delta q$ values were approximately equal to about 0.01–0.02 for all three kinds of processing surfaces. In other words, if the amount of feed per tooth is increased, Ra will increase. However, since the tip form of a cutter is the same, $R\Delta q$ does not change. For the shaper, the $R\Delta q$ value of the specimen is high for the two values of Ra that are $0.5\,\mu m$ or higher. This can be attributed to the curvature of a processing byte's cutting edge.

Figure 3 shows the relationship between the arithmetical mean roughness, Ra, and the glossiness of each surface. When the results for two of the processing methods were compared, the surface processed by vertical milling exhibited a slightly lower glossiness than the surface processed by horizontal milling. The glossiness of the shaper-processed surfaces was equal to or less than half of that for the milled surfaces. For vertical milling, the surface glossiness tends to decrease with a reduction in Ra.

To characterize the roughness profile of each specimen surface further, a frequency analysis was performed on the roughness profile of each surface. A fast Fourier transformation was applied to each surface's roughness profile data, and the number of waves per 1 mm length or f (spatial frequency) and the power spectral density (hereafter "PSD"), which represents the average energy per unit length, were
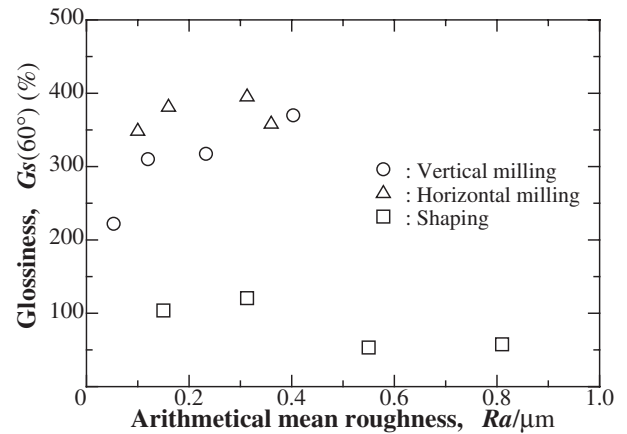
determined. PSD was calculated according to eq. (1). It should be noted that the number N of data points for each calculation is 8000.

$$PSD = P_x(k) = \frac{1}{KU} \sum_{r=1}^{K} |X_r(k)|^2 \qquad (1)$$

where K is the partition number at partial sequence $x_r(n)$ in data number $M (= 1024)$ of an N point sequence $x(n)$, and the partitioning of $x(n)$ is conducted by overlapping $M/2$ $(= 512)$. U is the energy of the data window $d(n)$ (hamming window) obtained from eq. (2).
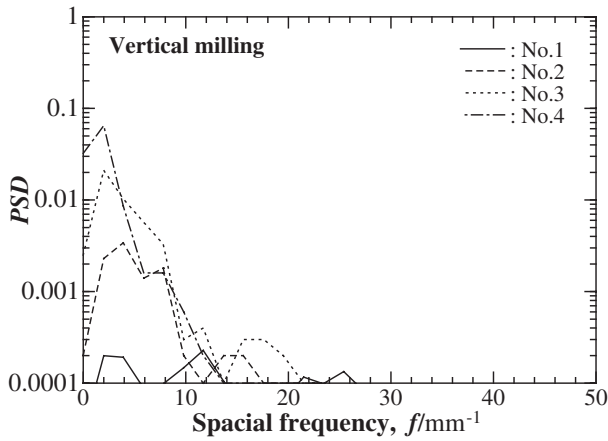
$$U = \sum_{n=0}^{M-1} d^2(n) \qquad (2)$$

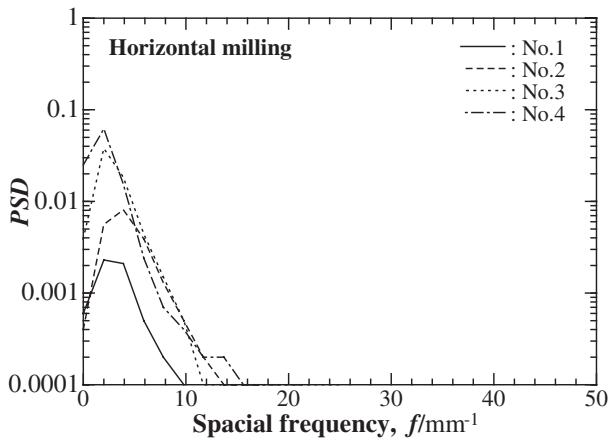$X_r(k)$ expresses each partial sequence $x_r(n)$ multiplied by data window $d(n)$.

Figures 4(a) through (c) reveal the relationship between the surface roughness profiles and their frequency analysis results. For the horizontally milled surface shown in Fig. 4(b), PSD was a maximum at $f \fallingdotseq 2\text{–}4\,mm^{-1}$, which was the maximum among all of the specimens. For the surface processed by the shaper, PSD took on a maximum at an f having a comparatively high value. A comparison of the data in Fig. 4 with the glossiness data in Fig. 3 suggests that the higher the surface glossiness, the lower the spatial frequency f at which the maximum surface PSD occurred. This indicates that the glossiness of a surface highly depends on the spatial frequency of its roughness profile.

The glossiness data in Fig. 3 indicates that the glossiness of specimen No. 1 was the lowest for all of the vertically milled surface specimens. Figure 4(a) displays the analysis results for the vertically milled surfaces. The PSD values for vertically milled specimen No. 1 at $f \fallingdotseq 2\text{–}3\,mm^{-1}$ and $f \fallingdotseq 12\,mm^{-1}$ were nearly equal. In addition, the surface indentations comprise low and high frequency components each having the same intensity. Because of this, the surface in question scatters a large fraction of incidental light, thereby giving it a low glossiness, since the glossiness is defined as the fraction of specular reflected light.

(a) Vertical milling

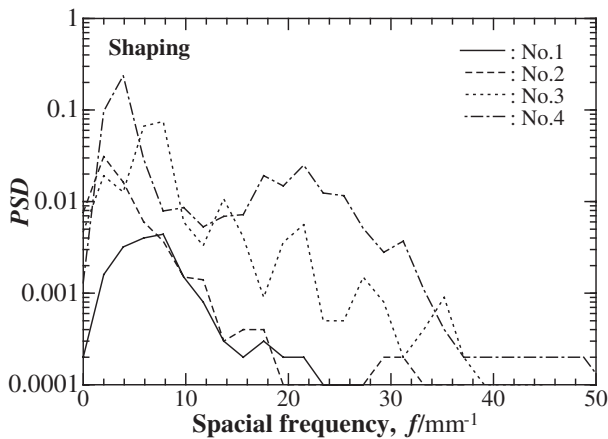

(b) Horizontal milling

(c) Shaping

Fig. 4 Power spectrum density of surface topography of specimens: (a) Vertical milling, (b) Horizontal milling and (c) Shaping.

Fig. 5 Effect of arithmetical mean roughness Ra on lightness L^* and specular reflectance $Gs(60°)/10$.

Table 3 The values of a, b and c of the approximation formulas for the effect of Ra on L^* and $Gs(60°)/10$, respectively. $\hat{y} = ax^b + c$

		a	b	c
Vertical milling	L^*	48.069	−0.079	0
	$Gs(60°)/10$	−48.069	−0.079	86
Horizontal milling	L^*	83.397	0.016	0
	$Gs(60°)/10$	−83.397	0.016	118.3
Shaping	L^*	74.765	0.067	0
	$Gs(60°)/10$	−74.765	0.067	78.5

The specular reflectance was obtained as follows. It is known that light impinging at an incident angle of 60° and specular reflected at 10% onto a reference surface (for a glass surface having a refractive index of 1.567) of a gloss meter gives a glossiness $Gs(60°) = 100\%$. From this, the specular reflectance was obtained by dividing the glossiness data $Gs(60°)$ by 10.

The curves in the figure represent regression curves relating Ra with L^*, and with the fraction of specular reflectance. The relationship between Ra and L^* was expressed by a regression line based on the least-square method. The relationship between Ra and the specular reflectance was determined as follows. Since it is known that the lightness L^* of a surface is linearly symmetrical to the fraction of specular reflected by the surface, a regression line was drawn between the two parameters based on the least-square method using the regression line between Ra and the lightness L^*. The coefficients, indices and constants defining these regression lines are cited in Table 3.

The results shown in Fig. 5 indicate that the surface processed by horizontal milling produces the highest lightness value. In fact, the surface looked whiter than the surfaces processed by vertical milling or the shaper. The specular reflectance and lightness L^* were linearly symmetrical with a 40–45% line as a boundary for the vertically milled and shaped surfaces. For the horizontally milled surface, however, the two parameters were linearly symmetrical with a 60% line as a boundary. In other words, although the specular reflectance changes similarly with Ra for the surfaces processed by vertical and horizontal milling, the lightness

3.2 Relationship between surface roughness and color

The study concerning the color of the specimen surfaces first focused on the relationship between the arithmetical mean roughness, Ra, and the lightness L^*. Figure 5 depicts the relationships between Ra and the lightness L^* of each surface, and between Ra and the specular reflectance.
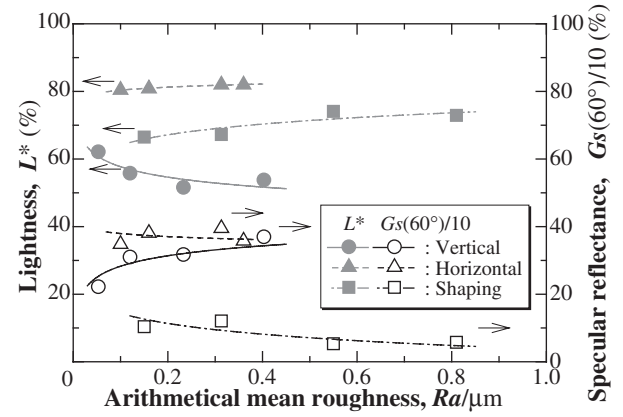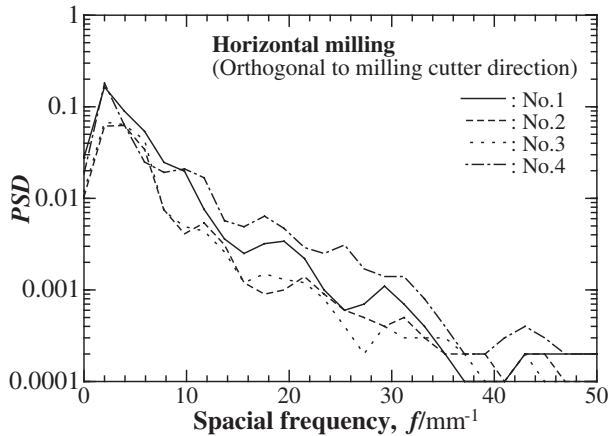
Fig. 6   Power spectrum density of surface topography in the direction orthogonal to the milling cutter direction.

Fig. 7 a^*, b^* chromaticity diagram.

change of the horizontally milled surface is larger by about 20–30 units than a corresponding change observed for the vertically milled surface.

This fact is due to the large coarseness that perpendicularly intersects the cutting direction, and originates from the diffusion reflection of the incident light. In glossiness measurement, light is irradiated from one direction. In the surface color measurements, however, the light is equally irradiated from all directions. Namely, a surface color measurement determines the light that carried out by diffusion reflection in the many directions while glossiness measurements only measure the light of a specular-reflected single direction.

Roughness was seen in the cutting direction (which perpendicularly intersects the feeding direction of the table) for the horizontally milled surface in this experiment. The arithmetical mean roughness value, Ra, of the roughness seen in this rectangular direction was about 0.6–0.7 mm. It is thought that this roughness was transferred from the blade during cutting.

Next, a frequency analysis on the roughness profile in the direction perpendicular to the cutting direction was carried out. The analysis results are shown in Fig. 6. Four kinds of specimens exhibited almost the same waveform, and the minute roughness along the edge of a blade was assumed to have transferred to the surface while cutting. Furthermore, a comparison of the roughness along the cutting direction shown in Fig. 4(b) reveals that the spatial frequency is high and the cycle of the transferred roughness was short. Therefore, it was better to use the surface color value rather than the glossiness value to characterize the surface texture of a surface that has a perpendicularly-oriented coarseness.

Figure 7 shows an a^*b^* color coordinate system which represents a color in terms of its hue (color spectrum corresponding, for example, red, blue or green) and chromaticness (vividness of color). A dot positioned more positively along the horizontal axis of the a^*b^* color coordinate system represents a redder hue, while a dot positioned more negatively along the same axis represents a greener hue. A dot positioned more positively along the vertical axis of the same system represents a more yellow hue, while a dot
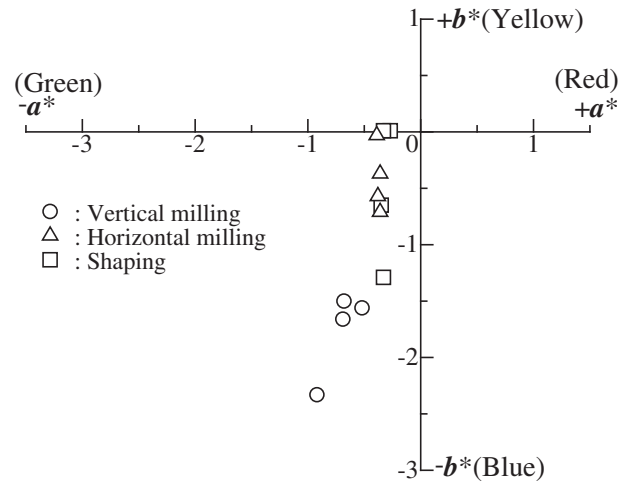
positioned more negatively along the same axis represents a bluer hue. In addition, the circle around the original point represents the color spectra. As a dot moves farther away from the original point, the color becomes more vivid. Conversely, the closer a dot is to the original point, the more dull or achromatic the color becomes.

Figure 7 reveals that the surface colors obtained from the processed surfaces are all located close to the original point, that is, all of the surfaces appear achromatic.[17] Moreover, the surface color values for all of the processed surface were located in the third quadrant. Therefore, although the surfaces were nearly colorless, they all appeared slightly blue.

4.   Conclusions

In this study, the surfaces of aluminum alloy A5052 specimens were processed by vertical milling, horizontal milling or shaping to obtain surfaces with three different textures. Each processing method was adjusted to produce three surfaces with sequentially increasing mean roughness, Ra, values. These specimen surfaces were then used to investigate the effect of surface roughness on the glossiness and color of the surface. The conclusions obtained from this study are cited below. The surface texture comparisons were performed using surfaces having approximately the same Ra values.

(1) The vertically milled surface and the horizontally milled surface produced nearly the same concavo-convex cycle and glossiness values. On the other hand, the concavo-convex cycle of a shaper-processed surface was short and the glossiness was lower, less than half of the milled surface values.

(2) The horizontally milled surface generated the highest lightness L^*, causing it to appear whiter than the surfaces processed by vertical milling or shaping. Since this surface contains roughness value in two directions that intersect perpendicularly, this characteristic can be attributed to the diffusion reflection of much light. That is, evaluation of the surface texture as a field was possible using the value of lightness L^*.

(3) The surface color of surfaces processed by vertical milling, horizontal milling and shaping all appear achromatic. These values, however, were all located in the third quadrant on the a^*b^* color coordinate system, indicating that the surfaces have a slightly bluish hue.

These experimental results will serve as a reliable indicator for those seeking a specific surface processing method that can confer an add-value to the surface texture.

Acknowledgement

REFERENCES

1) *Nikkei design*, (Nikkei Business Publications. Inc., Japan, **5**, 2003) pp. 66–71.
2) *Nikkei design*, (Nikkei Business Publications. Inc., Japan, **6**, 2004) pp. 46–58, 68–73.
3) J. Nara: J. JSPE. **42** (1976) 1088–1095.
4) A. Torao and M. Okuno: J. JSTP. **41** (2000) 648–652.
5) N. Arai, T. Toeda, H. Oguma and H. Shindo: SAITEC Report **1** (1999) 5–9.
6) *Processing Technique Data File*, (Technical Research Inst. JSPMI. Japan, **2**, 1977) 15/25.
7) H. E. Bennett and J. O. Porteus: J. Opt. Soc. Am. **51** (1961) 123–129.
8) J. H. Rakels: SPIE. **1009** (1988) 119–125.
9) S. V. Gils, S. Holten, E. Stijns, M. Vancaldenhoven, H. Terryn and L. Mattsson: Surf. Interface Anal. **35** (2003) 121–127.
10) M. Yonehara, T. Matsui, K. Kihara, H. Isono, A. Kijima and T. Sugibayashi: Mater. Trans. **45** (2004) 1027–1032.
11) T. Minoda, H. Hayakawa and H. Yoshida: J. JILM. **50** (2000) 491–494.
12) H. Yae, R. Kimura, M. Yoshida, G. Sasaki, J. Pan, K. Yokoyama and H. Fukunaga: J. JILM. **52** (2002) 303–307.
13) M. Yonehara, T. Matsui, K. Kihara, H. Isono, A. Kijima and T. Sugibayashi: Mater. Trans. **45** (2004) 1019–1026.
14) T. R. Thoman and G. Charlton: ASPE. **3** (1981) 91–96.
15) JIS H 4000:1999.
16) JIS B 0105:1993.
17) M. Yonehara, K. Kihara, H. Isono, A. Kijima, S. Yoshimori and T. Sugibayashi: J. JRI Cu. **42** (2003) 340–344.